ChemPubSoc Europe

DOI: 10.1002/cplu.201402026

Silver Coordination Polymers Based on *p*-Cyanophenylsilanes as Ligands

Bianca Blankschein,[a] Axel Schulz,*[a, b] Alexander Villinger,[a] and Ronald Wustrack[a]

Dedicated to Professor Ingo-Peter Lorenz on the occasion of his 70th birthday

Differently substituted *p*-cyanophenylsilanes, $Me_{4-n}Si(C_6H_4CN)_n$, ($n=2$, 3, 4), $PhSi(C_6H_4CN)_3$, $cycHexSi(C_6H_4CN)_3$ (cycHex = cyclohexyl), and $MePhSi(C_6H_4CN)_2$, were prepared and fully characterized. Their coordination behavior was studied by utilizing silver salts of the type AgX ($X=O_3SCF_3^-$, $CO_2CF_3^-$), which led to coordination polymers. One-dimensional chains were observed for the bidentate *p*-cyanophenylsilane ligands, whereas two- and three-dimensional networks, including macrometalacycles, were found for the tridentate ligand. Treatment of AgO_2CCF_3 with the tetradentate ligand $Si(C_6H_4CN)_4$ led to the formation of a diamond-like three-dimensional network with two interpenetrating nets linked by bridging $Ag_2(CF_3CO_2)_2$ dimers. X-ray structures show a wide range of close Ag···Ag distances in the polymers, which are dependent on the ligand and the anion utilized.

Introduction

In recent years, there has been increasing interest in metal-containing coordination polymers. Their topological diversity makes them interesting for versatile applications.[1–9] In most cases, the resulting topology is unpredictable and can be influenced by many factors. Besides the ligand and metal center, the coordination behavior of the anion,[10–13] solvent molecules,[14,15] or the ratio[16] of metal salt and ligand can also change the topology of the network.

This study presents a series of different *p*-cyanophenylsilanes as ligands and their application and function in network formation. For the last five years, we have been dealing with novel CN-based anions (e.g., $[Al(O–C_6H_4–CN)_4]^-$) and their application as weak coordinating anions for the generation of ionic liquids.[17–20] We were intrigued by the idea to use neutral *p*-cyanophenylsilanes, which are formally isolobal to $[Al(O–C_6H_4–CN)_4]^-$ (Al^- substituted by Si). The use of silicon-based cyano compounds is interesting because they are robust and the starting materials are available in large quantity at low cost. In comparison to the analogous carbon compounds, the larger Si–C distance relative to the C–C distance makes these ligands structurally more flexible.[21] In recent years, many examples of silicon-based ligands have been published;[22–29] however, to the best of our knowledge, only two examples of coordination polymers with *p*-cyanophenylsilanes and silver centers have been reported. In 1997, Tilley and Liu described coordination polymers generated from $Si(C_6H_4CN)_4$ and AgOTf (OTf = O_3SCF_3) as well as $AgPF_6$.[30] Herein, we describe in detail the influence and structural diversity of silver coordination compounds dependent upon the anion ($O_3SCF_3^-$ and $CO_2CF_3^-$) and differently substituted neutral *p*-cyanophenylsilanes. For this, we started with the preparation of $Me_{(4-n)}Si(p\text{-}C_6H_4CN)_n$ ($n=1$–3) and their silver salts. To study the influence of the methyl group on the structure, we also prepared $Ph_{(4-n)}Si(p\text{-}C_6H_4CN)_n$ ($n=2$, 3), $cycHexSi(p\text{-}C_6H_4CN)_3$ (cycHex = cyclohexyl), and their silver salts.

[a] B. Blankschein, Prof. Dr. A. Schulz, Dr. A. Villinger, Dr. R. Wustrack
Universität Rostock, Institut für Chemie
Albert-Einstein-Strasse 3a, 18059 Rostock (Germany)

[b] Prof. Dr. A. Schulz
Leibniz-Institut für Katalyse e.V. an der Universität Rostock
Albert-Einstein-Strasse 29a, 18059 Rostock (Germany)
E-mail: axel.schulz@uni-rostock.de

Supporting information for this article is available on the WWW under http://dx.doi.org/10.1002/cplu.201402026.

Results and Discussion

Synthesis of ligands

Generally, there are two different synthetic routes to *p*-cyanophenylsilanes of the type $R_{(4-n)}Si(p\text{-}C_6H_4CN)_n$ (R = Me, Ph; $n=1$–4). 1) As shown by van Walree et al.,[31] $Me_3Si(p\text{-}C_6H_4CN)$ and $Me_2Si(C_6H_4CN)_2$ were prepared from lithiated 1,4-dibromobenzene (BrC_6H_4Br) and the corresponding chlorosilane, R_3SiCl, leading to the formation of bromophenylsilane, $R_3Si–C_6H_4Br$, which gave the desired cyano compound, $R_3Si–C_6H_4CN$, after the addition of CuCN. 2) Tilley and Liu obtained $Si(C_6H_4CN)_4$ directly from BrC_6H_4CN after lithiation and addition of $SiCl_4$ (Scheme 1).[30] We preferred the second approach because the method by van Walree did not seem to be applicable for higher substituted cyanosilanes. A major challenge of the approach by Tilley and Liu arises from lithiation of the cyano group, which competes with the desired lithium–halogen exchange at the phenyl ring; this was intensively studied by Parham and Jones in the 1970s.[32] In contrast to Tilley and Liu, we therefore decided to dramatically decrease the reaction time and kept the reaction mixture always below −80 °C. This protocol prevents *n*BuLi from reacting with the CN triple bond.

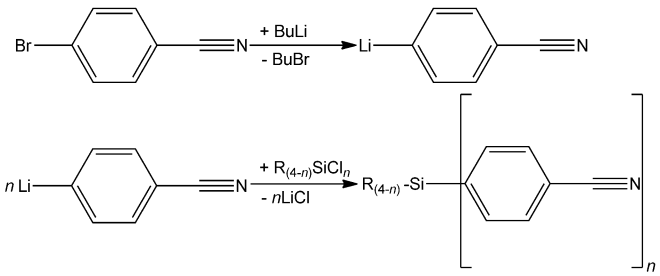

Scheme 1. General synthesis of *p*-cyanophenylsilanes of the type $R_{(4-n)}Si(p\text{-}C_6H_4CN)_n$ (R = Me, Ph, etc.; n = 1-4).

Because the product, $R_{(4-n)}Si(p\text{-}C_6H_4CN)_n$, is water stable, further reactions and the formation of side products at elevated temperatures was avoided by adding water to decompose remaining or excess *n*BuLi. In addition to the decomposition of excess *n*BuLi, lithium chloride, which is also formed in the reaction, can easily be separated (Scheme 1).

By this modified synthetic route, all *p*-cyanophenylsilanes of the type $Me_{4-n}Si(p\text{-}C_6H_4CN)_n$ (n = 1, 2, and 4) and novel $RSi(C_6H_4CN)_3$ (R = Ph, Me, cycHex) were obtained in moderate to good yields (between 10 and 65 %). All ligands were fully characterized by means of elemental analysis; ^{1}H NMR, ^{13}C NMR, ^{29}Si NMR, IR, and Raman spectroscopy; and X-ray structure elucidation. These data are summarized in Table 1. All prepared *p*-cyanophenylsilanes (species **1**–**5**, Table 1) are neither air nor moisture sensitive, can be prepared in bulk, and are almost indefinitely stable when stored in a sealed tube. They are thermally stable up to over 300 °C and melt between 101 (**1**) and 270 °C (**5**).

Table 1. Experimental data for *p*-cyanophenylsilanes **1**–**4**.[a]

	Yield [%]	M.p. [°C]	δ^{13}C (CN) [ppm]	δ^{29}Si [ppm]	$\tilde{\nu}_{IR}$CN [cm^{-1}]	$\tilde{\nu}_{Raman}$CN [cm^{-1}]
Me_2SiY_2 (**1**)	53	101	118.9	−5.96	2224 (m)	2226(10)
$MeSiY_3$ (**2**)	10	119	118.7	−9.35	2228 (s)	2230(10)
$PhSiY_3$ (**3**)	26	192	118.7	−14.17	2229 (m)	2230(10)
$cycHexSiY_3$ (**4**)	52	183	118.7	−10.23	2227 (m)	2229(10)
SiY_4 (**5**)	65	270	118.5	−14.09	2228 (s)	2231(10)

[a] Y = $-C_6H_4CN$.

The NMR spectroscopy data illustrate very similar ^{13}C chemical shifts between δ = 118.5 and 118.9 ppm, whereas ^{29}Si NMR spectroscopy can be used to distinguish between alkyl and phenyl substitution, as well as displaying different degrees of substitution. According to the observed IR and Raman data, the stretching mode of the CN groups was detected in the typical region between $\tilde{\nu}$2224 and 2231 cm^{-1}[17–20] and could not be utilized to distinguish between species **1**–**5** in Table 1.

Reaction of AgX (X = CF_3SO_3, CF_3CO_2) with *p*-cyanophenylsilanes

Synthesis of $[Ag\{Me_2Si(C_6H_4CN)_2\}]X$ (X = CF_3SO_3 (6), CF_3CO_2 (7))

The silver triflate and trifluoroacetate salts of the $Me_2Si(C_6H_4CN)_2$ ligand are easily obtained in the reaction of AgX in CH_2Cl_2 (suspension) with $Me_2Si(C_6H_4CN)_2$ within 1 h in good yields (yields: 70 (**6**), 64 % (**7**)).

Synthesis of $[Ag\{RSi(C_6H_4CN)_3\}]CF_3SO_3$ (R = Me (8), Ph (10), and cycHex (12)) and reaction of $AgCF_3CO_2$ with $RSi(C_6H_4CN)_3$ (R = Me (11), Ph (13))

All three triply substituted triflate silver coordination polymers were obtained within 1 h from a stirred solution of silver triflate in benzene (10 mL) after the addition of $RSi(C_6H_4CN)_3$ dissolved in benzene. The concentration of these solutions often gave viscous colorless oils, from which **8**, **10**, and **12** crystallized in moderate yields (30–40 %). Interestingly, although for the reaction of $AgCF_3CO_2$ with $PhSi(C_6H_4CN)_3$ a salt of the type $[Ag\{PhSi(C_6H_4CN)_3\}]CF_3CO_2$ (**11**) was observed (yield 48 %), the analogous reaction with $MeSi(C_6H_4CN)_3$ led to the formation of $[(Ag\{MeSi(C_6H_4CN)_3\})_2][Ag_4(CF_3CO_2)_6]$ (**13**), which exhibited a silver-containing complex anion (Scheme 2). This reaction was then optimized, with respect to the stoichiometry, which gave finally **13** in good yields (51 %).

Reaction of AgX with $Si(C_6H_4CN)_4$ (X = CF_3SO_3, CF_3CO_2)

In 1997, Tilley and Liu reported on the synthesis of $[(Ag_2\{Si(C_6H_4CN)_4\})_2][CF_3SO_3]_2$·2 benzene (**14**·2 benzene), which was afforded from a solution of $AgCF_3SO_3$ in benzene layered with $Si(C_6H_4CN)_4$ dissolved in CH_2Cl_2.[30] A similar approach was used for silver trifluoroacetate. However, crystalline material was only obtained if the mixture of $AgCF_3CO_2$ $Si(C_6H_4CN)_4$ in benzene was boiled under reflux for 30 min followed by slow

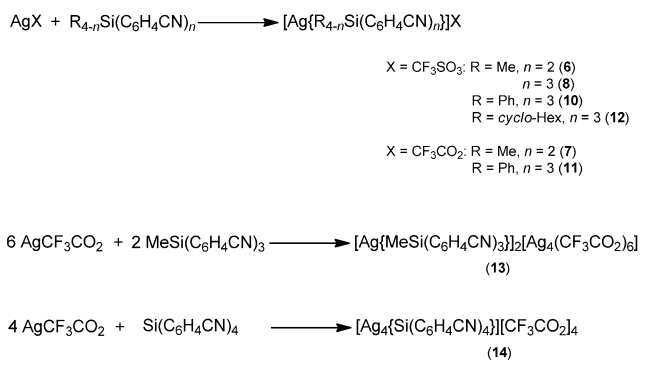

Scheme 2. Generation of silver coordination polymers in the reaction of AgX with several *p*-cyanophenylsilanes.

cooling to room temperature (yield 42%. X-ray studies of these colorless crystals revealed the presence of **13**.

Properties and spectroscopic characterization

All silver coordination polymers described herein are air stable, but slowly decompose in water. The IR and Raman data of all considered species in Table 2 show sharp bands in the expected region $\tilde{\nu}$2236–2254 cm^{-1}, which can be assigned to the ν_{CN} stretching frequencies. As previously shown, the coordination of Lewis acids, such as $B(C_6F_5)_3$, or cationic metal centers to a NC–R species causes a significant band shift to higher wavenumbers.[33] Hence, both IR and Raman spectroscopy are particularly well suited to distinguish between metal–CN-coordinated *p*-cyanophenylsilanes and the naked *p*-cyanophenylsilane molecule with shifts between $\tilde{\nu}$7 and 32 cm^{-1} to higher wavenumbers in the silver coordination polymers. Uncoordinated CN groups, such as those in compound **11**, are also easily spotted. The shift to higher wavenumbers upon metal coordination correlates nicely with a slightly smaller C–N distance (Table 2).

Table 2. Wavenumbers [cm^{-1}] of $\tilde{\nu}_{CN}$ in the coordination polymers, along with Ag–N, Ag–O, and Ag···Ag distances [Å].

	6	7	8	13	10	11	12	14
$\tilde{\nu}_{IR}$	2254	2236	2249	2250	2250	2248, 2231[b]	2249	2254, 2235
$\tilde{\nu}_{Raman}$	2254	2243	2262	2253	2252	2229[b]	2254	2259, 2243
$\Delta\tilde{\nu}_{IR}$[a]	30	12	21	22	21	19, 2[b]	22	26, 7
$\Delta\tilde{\nu}_{Raman}$[a]	28	17	32	23	22	1[b]	25	28, 12
Ag–N	2.207(3) 2.241(3)	2.361(3) 2.397(3)	2.226(4) 2.268(4) 2.288(4)	2.194(2) 2.238(2) 2.292(2) 2.637(2)	–[c]	2.279(6) 2.291(5)	2.210(2) 2.237(2) 2.311(2)	2.272(5) 2.233(4)
Ag–O	2.472(2) 2.837(7) 2.84(1)	2.277(2) 2.300(8)	2.595(8)	2.185(5) 2.235(2) 2.317(2) 2.232(4) 2.324(2)	–[c]	2.293(6) 2.354(8)	2.388(9)	2.284(3) 2.207(4) 2.219 (4) 2.392(3) 2.366(3)
Ag···Ag	4.3892(4)	3.0657(6)	14.047(3)	2.9708(3) 3.0826(3) 3.1033(3) 3.1091(4)	–[c]	3.173(1)	14.5496(3)	3.3039(4) 2.9512(7) 3.5024(7)

[a] Compared with the naked ligand molecule, see Table 1. [b] Uncoordinated CN group. [c] Poor data set.

X-ray crystallography

To further evaluate the influence of the counterions on the structure of the complexes, the more strongly coordinating anion $CF_3CO_2^-$ (TFA) was used in the reaction with *p*-cyanophenylsilanes for comparison with structures with weakly coordinating $CF_3SO_3^-$ (OTf) anions. The structures of all utilized *p*-cyanophenylsilanes, $RSi(p\text{-}C_6H_4CN)_3$ (with R = Ph, Me, cycHex) and $Si(p\text{-}C_6H_4CN)_4$, as well as silver salts **6**–**8** and **10**–**14**, determined. Tables S1–S6 present the X-ray crystallographic data; selected molecular parameters are listed in Tables S7–S18 in the Supporting Information. X-ray quality crystals of all considered species were selected in Fomblin YR-1800 (Alfa Aesar) at ambient temperature. All samples were cooled to 173 K during the measurements.

p-*Cyanophenylsilanes*

Apart from species **4**·benzene, all other considered *p*-cyanophenylsilanes (Figure 1) crystallized free from benzene and CH_2Cl_2. (Crystallization of pure **4** from thf leads to the formation of **4**·thf.) Although in all structures the molecules are well-separated from each other, there are numerous very weak H_{aryl}···N–C and H_{aryl}···$C_{phenyl,alkyl}$ interactions in the range between 2.4 and 3.0 Å. The silicon atom in all *p*-cyanophenylsilanes is tetrahedrally coordinated with bonding angles around the silicon atoms of 105.2–111.4° (**2**), 106.2–112.7° (**3**), 104.7–112.6° (**4**), and 106.4–111.8° (**5**); these values display a significant deviation from an ideal tetrahedral environment. The Si–C distances all lie in the expected range 1.859(1)–1.886(1) (**2**), 1.869(2)–1.884(2) (**3**), 1.877(1)–1.880(1) (**4**), and 1.874(1)–1.878(1) Å (**5**); this indicates typical S–C single bonds (cf. Σr_{cov}(Si–C) = 1.91 Å).[34] The average CN distances amount to 1.145(2) (**2**), 1.144(2) (**3**), 1.144(2) (**4**), and 1.143(2) (**5**, cf. Σr_{cov}(C≡N) = 1.14 Å).[34]

Coordination polymers with the bidentate ligand $Me_2Si(p\text{-}C_6H_4CN)_2$

$^1{}_{\infty}\{[Ag\{Me_2Si(p\text{-}C_6H_4CN)_2\}]O_3SCF_3\cdot CH_2Cl_2\}$ (**6**·CH_2Cl_2) crystallizes in the orthorhombic space group *Pnma* with eight formula units per cell. Each Ag^+ ion is surrounded by two neutral $Me_2Si(p\text{-}C_6H_4CN)_2$ ligands, which coordinate to Ag^+ through one nitrogen atom of the CN group (Ag1–N1 2.241(3) and Ag1–N2 2.207(3) Å (cf. r_{cov}(Ag–N) = 1.99 Å)), and two triflate ions, which each coordinate through one oxygen atom (Ag1–O4 2.472(2) Å) and two oxygen atoms (Ag–O2 2.84(1), Ag1–O3 2.827(7) Å). Only weak van der Waals interactions can be expected along the Ag···O5 (3.222(3) Å) units. Although the N2-Ag1-N1 angle is rather large at 127.6(1)°, all other angles around the Ag^+ ion are smaller than 100° (e.g., O3-Ag1-O4 73.1(2)°, O2-Ag1-O3 51.3(2)°). It should be noted that one triflate anion (around S1) is disordered over two positions. Because one oxygen atom (O1, O3) of both triflate anions act as bridging ligand atoms, the formation of $Ag_2(OTf)_2L_2$ (L = $Me_2Si(p\text{-}C_6H_4CN)_2$) dimers as the smallest building block is observed (Figures 2 and 3). As depicted in Figure 3, the remaining CN group of the $Me_2Si(p\text{-}C_6H_4CN)_2$ ligand connects this dimer

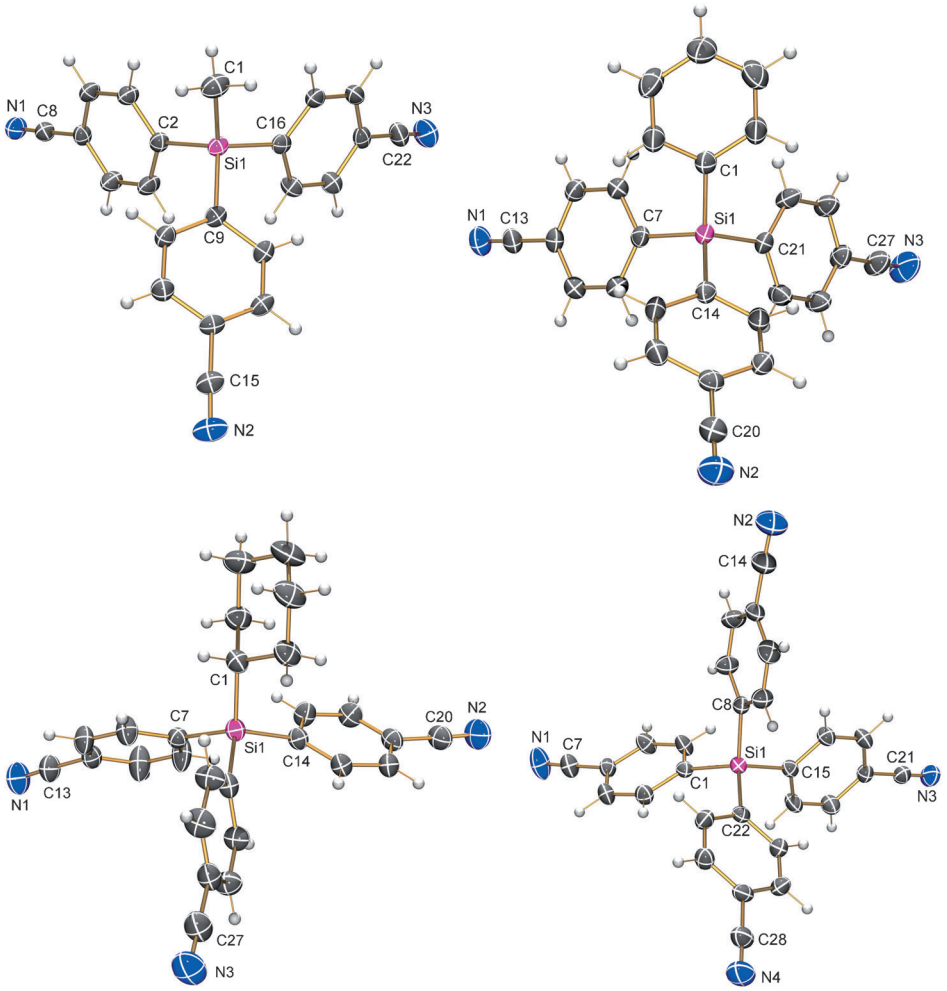

Figure 1. ORTEP drawing of the molecular structure of $MeSi(C_6H_4CN)_3$ (top left, **2**), $PhSi(C_6H_4CN)_3$ (top right, **3**), $cycHexSi(C_6H_4CN)_3$ (bottom left), and $Si(C_6H_4CN)_4$ (bottom right) in the crystal. Thermal ellipsoids with 50% probability at 173 K. Selected bond lengths [Å]: **2**: Si1–C1 1.859(1), Si1–C9 1.880(1), Si1–C2 1.881(1), Si1–C16 1.886(1), N1–C8 1.144(2), N2–C15 1.143(2), N3–C22 1.149(2); **3**: Si1–C1 1.869(2), Si1–C14 1.876(2), Si1–C7 1.881(2), Si1–C21 1.884(2), N1–C13 1.142(2), N2–C20 1.147(3), N3–C27 1.143(2); **4**·benzene (benzene not shown for clarity): Si1–C14 1.877(1), Si1–C1 1.877(2), Si1–C21 1.879(1), Si1–C7 1.880(1), N1–C13 1.141(2), N2–C20 1.143(2), N3–C27 1.144(2); **5**: Si1–C1 1.878(2), Si1–C8 1.871(2), Si1–C15 1.876(2), Si1–C22 1.874(2), N1–C7 1.143(2), N2–C14 1.147(3), N3–C21 1.140(2), N4–C28 1.142(2).[56]

tate ligands.[35–37] One CH_2Cl_2 solvent molecule per $[Ag\{Me_2Si(p\text{-}C_6H_4CN)_2\}]O_3SCF_3$ unit is found between these chains.

$^1{}_\infty\{[Ag\{Me_2Si(p\text{-}C_6H_4CN)_2\}]O_2CCF_3\cdot 0.5\,CH_2Cl_2\}$ (**7**·0.5 CH_2Cl_2) also crystallizes in the orthorhombic space group *Pnma* with eight formula units per cell, but with half of a CH_2Cl_2 molecule per formula unit. Similar to **6**·CH_2Cl_2, the TFA anion and $Me_2Si(C_6H_4CN)_2$ act as bidentate ligands. Although the chelating TFA anions are responsible for the formation of a $Ag_2(TFA)_2$ dimer (Figure 4), the $Me_2Si(C_6H_4CN)_2$ ligand links these silver dimers to double-stranded chains, leading to a 1D coordination polymer, as shown in Figure 5. It is worth noting that the TFA anion is capable of exhibiting different coordination modes, as shown in Scheme 3.[38]

The Ag^+ ions sit in a strongly distorted tetrahedral environment with local C_{2v} symmetry, rather large O1-Ag1-O2 angles (154.2(2)°), and much shorter N1-Ag1-N2 angles (104.5(1)°), contrary to the situation found for **6**·CH_2Cl_2 (see above); this displays the high flexibility of the $Me_2Si(C_6H_4CN)_2$ ligand. Relative to **6**·CH_2Cl_2 the Ag–N bond lengths are considerably longer (**7**·0.5 CH_2Cl_2: Ag1–N1 2.397(3),

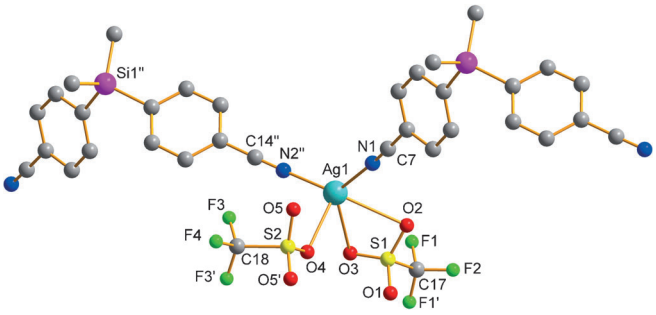

Figure 2. Ball-and-stick representation of the Ag^+ ion environment in **6**·CH_2Cl_2 (symmetry code: ′: *x*, 0.5−*y*, *z*; ″: 1+*x*, *y*, *z*). Disorder around S1 not shown. Hydrogen atoms are omitted for clarity.

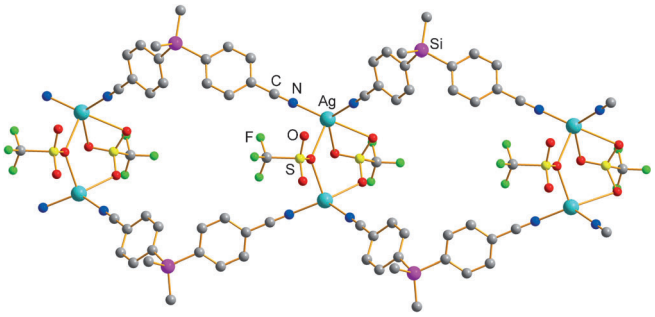

Figure 3. Ball-and-stick representation of a section of the double strand in **6**·CH_2Cl_2 (view along *c*-axis). Solvent molecules, which are located in the voids, are omitted.

to a chain in the unit cell. Hence, compound **6**·CH_2Cl_2 might be regarded as a 1D coordination polymer, which was described before in a number of structural reports utilizing biden-

Ag1–N2 2.361(3) Å vs. Ag1–N1 2.241(3), and Ag1–N2 2.207(3) Å in **6**·CH_2Cl_2), whereas the Ag–O distances are significantly shorter in **7**·0.5 CH_2Cl_2 (**7**·0.5 CH_2Cl_2: Ag1–O1 2.300(8),

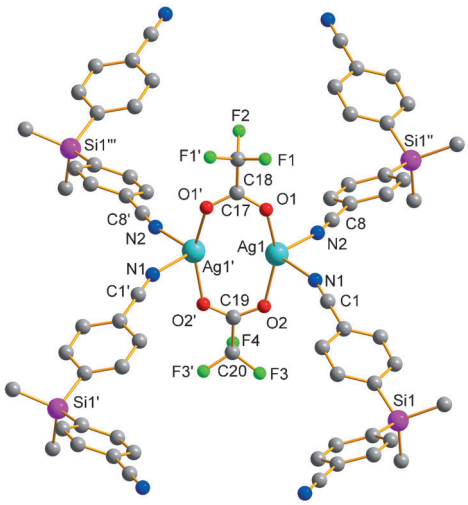

Figure 4. Ball-and-stick representation of the $Ag_2(TFA)_2Y_2$ dimer in **7**·0.5 CH_2Cl_2 (symmetry codes: ′: $x,1.5-y,z$; ″: $1+x,y,z$; ‴: $1+x,1.5y,z$). Disorder around C18 and C20 is not shown. Hydrogen atoms are omitted for clarity.

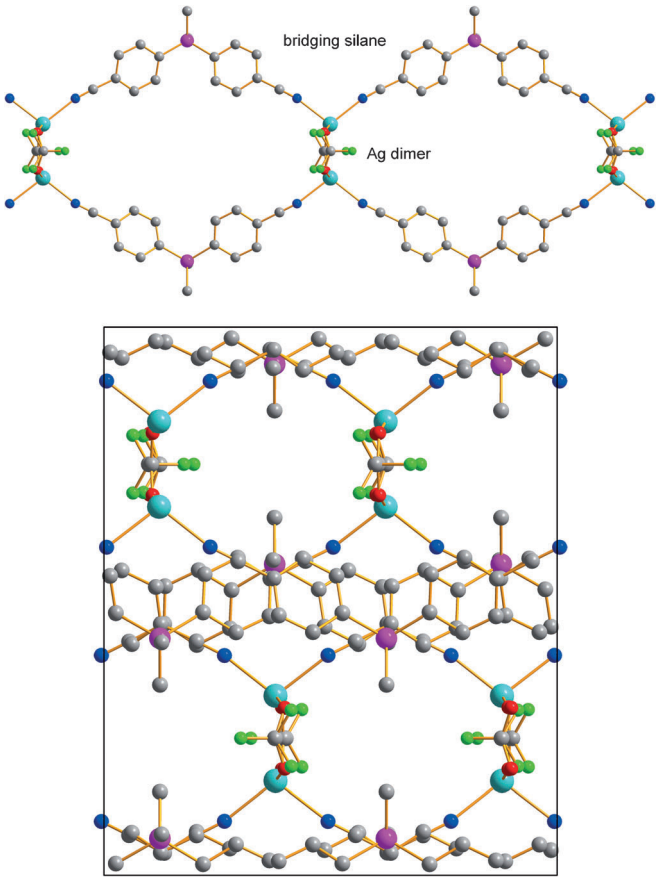

Figure 5. Ball-and-stick representation of a section of the double strand (top) and view of the cell along the *c* axis in **7**·CH_2Cl_2 (bottom). Solvent molecules, which are located in the voids, are omitted for clarity as well as all hydrogen atoms.

Ag1–O2 2.77(2) Å vs. Ag1–O4 2.472(2), Ag–O2 2.84(1), Ag1–O3 2.827(7) Å in **6**·CH_2Cl_2), which indicates stronger bonding between the TFA anion and the Ag^+ centers compared with the

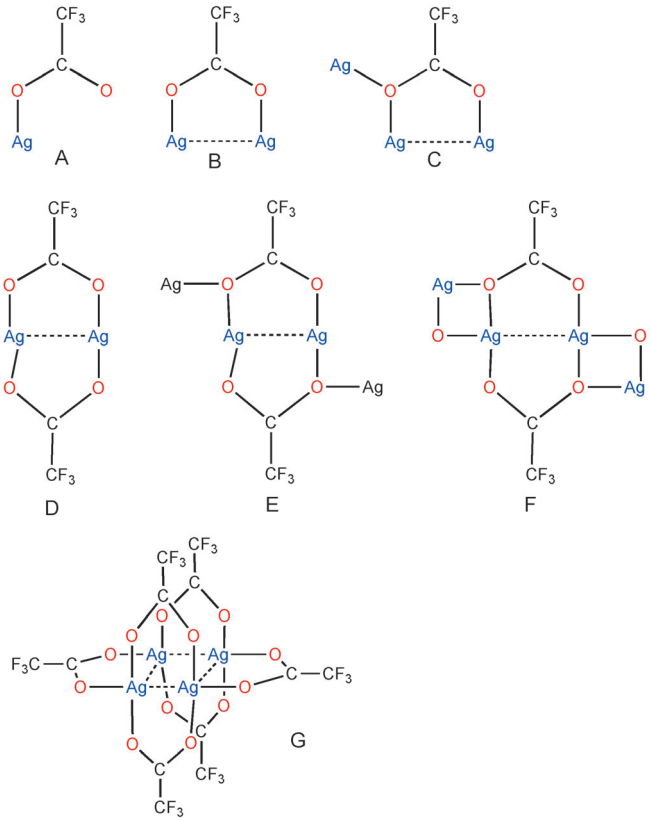

Scheme 3. Different coordination modes of the TFA anion.

OTf^- ion and the Ag^+ ions. Otherwise, the $Me_2Si(C_6H_4CN)_2$ ligand coordinates stronger to Ag^+ in **6**·CH_2Cl_2.

Coordination polymers with the tridentate ligand RSi(p-$C_6H_4CN)_3$ (R = Me, Ph, cycHex)

$^3{}_\infty\{[Ag\{MeSi(p\text{-}C_6H_4CN)_3\}]O_3SCF_3\cdot 2\,benzene\}$ (**8**·2 benzene) crystallizes in the monoclinic space group $P2_1/n$ with four formula units per cell. Voids are filled with benzene molecules (two per formula unit). As shown in Figure 6 (top left), the (distorted) tetrahedral coordination of each Ag^+ ion consists of three nitrogen atoms from three distinct $MeSi(p\text{-}C_6H_4CN)_3$ ligand molecules and one oxygen atom from the triflate group. Whereas all nitrogen atoms of the $MeSi(p\text{-}C_6H_4CN)_3$ ligand are involved in binding Ag^+ ions, leading to a 3D network, the triflate anion acts as monodentate ligand and two oxygen atoms remain uncoordinated. Because each CN group of $MeSi(p\text{-}C_6H_4CN)_3$ always links one Ag^+ ion and the $MeSi(p\text{-}C_6H_4CN)_3$ ligand acts as a bridging ligand, the formation of a macrocycle (repeat unit) can be observed. The repeat unit of the 3D coordination polymer is a 70-membered Ag^5L_5 macrocycle (L = $MeSi(C_6H_4CN)_3$; Figure 6, top left). Cross-linking between the macrocycles, which leads to the formation of a 3D network (Figure 6, bottom), is achieved by one cyano group per $MeSi(p\text{-}C_6H_4CN)_3$ ligand. In this macrometalacycle, the length of the sides are about 29.7 (transannular Ag···Si distance) and 16.7 Å (transannular Ag···Ag distance). A closer look at the 3D network revealed a highly interpenetrated structure for

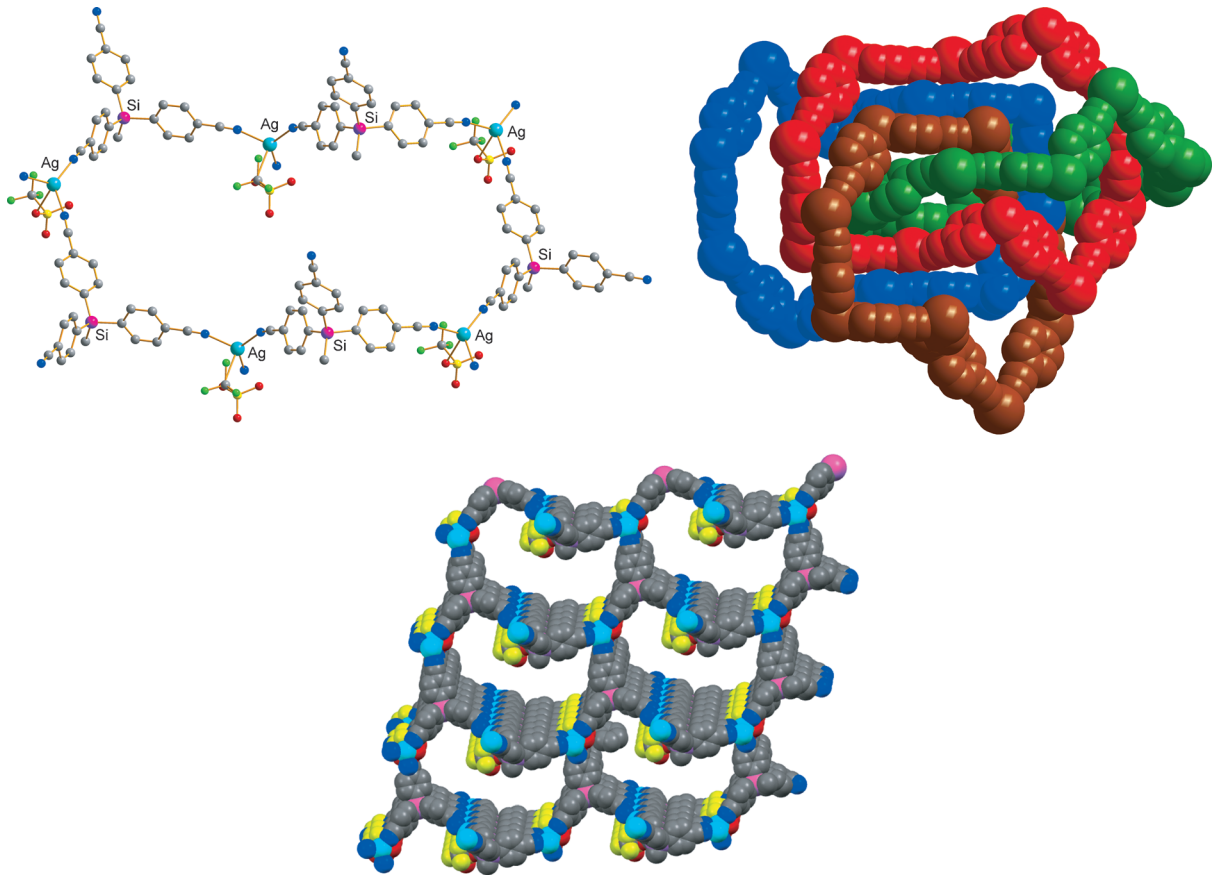

Figure 6. Ball-and-stick representation of one macrocycle (repeat unit) in **8**·2 benzene (top left), space-filling representation of four-fold interpenetration (top right) and one 3D network (without interpenetrating networks; bottom) built from the repeat unit via CN coordination. Solvent molecules, which are located in the voids, are omitted for clarity as well as all hydrogen atoms.

8·2 benzene, which does not possess large free channels or pores.[39–42] It consists of four independent infinite frameworks, each with the same topology as that discussed before (Figure 6, top right). Ni et al. described such a fourfold interpenetrated structure with four symmetry-equivalent frameworks for AgX (X = BF_4, ClO_4, CF_3SO_3) with tris(4-cyanophenyl)amine (TCPA).[43]

The Ag–N bond lengths range from 2.226(4) to 2.288(4) Å, which is slightly shorter than that observed in **7**·0.5 CH_2Cl_2, but in the range found in **6**·CH_2Cl_2. The Ag–O bond amounts to 2.595(8) Å, which is in accordance with those found for **6**·CH_2Cl_2 and **7**·0.5 CH_2Cl_2. The Ag···Ag distances are all larger than 11.79(9) Å; thus no metallophilic interactions are found (see above).

$^2{}_\infty\{[Ag\{MeSi(p\text{-}C_6H_4CN)_3\}]_2[Ag_4(O_2CCF_3)_6]\cdot 3.5\,benzene\}$ (**13**·3.5 benzene), which precipitates from a solution of AgO_2CCF_3 and $MeSi(p\text{-}C_6H_4CN)_3$, in contrast to **8**·2 benzene, crystallizes in the triclinic space group $\bar{P}1$ with two formula units per unit cell. Single-crystal analysis revealed three independent silver(I) centers (Scheme S10 in the Supporting Information): Ag1 is exclusively bound by nitrogen atoms, whereas Ag2 and Ag3 are exclusively linked by oxygen atoms of the carboxy group (Figure 7). Hence, in contrast to the triflate species **8**·2 benzene, $CF_3CO_2^-$ causes a 2D cationic network ($^2{}_\infty\{[Ag\{MeSi(p\text{-}C_6H_4CN)_3\}]_2{}^{2+}$) with large guest $[Ag_4(CF_3CO_2)_6]^{2-}$ anions (as well as solvent molecules) that are fixed in the cavities of the host networks for **13**·3.5 benzene (Figure 8). A similar situation was reported by Ni et al. for AgO_2CCF_3 with the tridentate ligand TCPA.[43]

Although the anion is different from that of **8**·2 benzene, the coordination mode by the bridging $MeSi(p\text{-}C_6H_4CN)_3$ ligand is the same as that observed in **13**·3.5 benzene; however, one nitrogen atom of $MeSi(p\text{-}C_6H_4CN)_3$ acts a μ^2-bridge, leading to the formation of a four-membered Ag_2N_2 ring in a centrosymmetric Ag_2N_6 dimer (Figure 7 left, Ag-N-Ag 77.86(6)°). For this reason, two types of Ag–N bond lengths are detected: three short distances ranging from 2.194(2) to 2.292(2) Å and one significantly longer distance of 2.637(2) Å (cf. r_{cov}(Ag–N) = 1.99 Å), which is considerably shorter than the sum of covalent radii (r_{vdW}(Ag···N) = 3.27 Å).[44] Therefore, coordination around Ag1 might be considered as a distorted trigonal arrangement (N-Ag-N 113.69(8), 121.42(9), and 123.44(8)°) or as a distorted tetrahedral (N-Ag-N 87.00(8), 92.70(8), and 102.14(6)°) in a [3+1] coordination mode. In addition, as depicted in Figure 6, transannular Ag···Ag interactions must be considered as well as Ag···Ag interactions between the silver centers of the cationic framework and the silver centers of the cluster anion; a very intriguing unprecedented structural feature, which is of interest with respect to the question of the dimensionality of the network (see above). The Ag···Ag distances be-

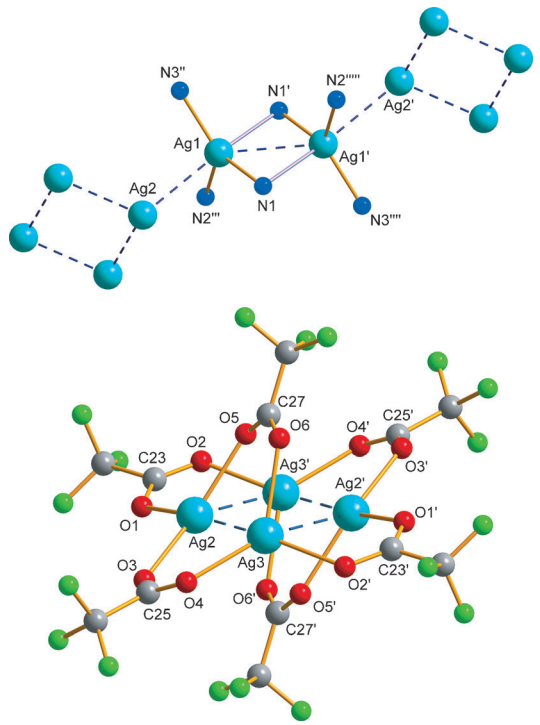

Figure 7. Ball-and-stick representation of the coordination sphere around $Ag1^{+}$ in the cationic framework (top; only the N atoms of the MeSi(*p*-$C_6H_4CN)_3$ ligands are shown) and the molecular cluster anion $[Ag_4(O_2CCF_3)_6]^{2-}$·(bottom) in **13**·3.5 benzene. Dashed lines represent Ag(d^{10})···Ag(d^{10}) van der Waals interactions. Symmetry codes: left, ′: $-x$, $1-y$, $1-z$; ″: x, $1+y$, z; ‴: x, y, $1+z$; ⁗: $-x$, $-y$, $1-z$; ′′′′′: $-x$, $1-y$, $-z$; right, ′: $1-x$, $1-y$, $1-z$.

tween 3.0826(3) ("interionic") and 3.1091(4) Å (transannular) are significantly shorter than the sum of the van der Waals radii of two silver atoms (3.42 Å[44]) and are comparable to those found in other structurally characterized $AgCF_3CO_2$ complexes.[45,46]

Starting from the distorted trigonal AgN_3 unit (Figure 7, left), each MeSi(*p*-$C_6H_4CN)_3$ ligand links three Ag1 atoms to generate an infinite honeycomb network.[47,48] The 3 Ag1 ions and 3 MeSi(*p*-$C_6H_4CN)_3$ ligands (each MeSi(*p*-$C_6H_4CN)_3$, using two of the three arms, connects two silver atoms in each macrocyclic unit) form a 48-membered (Ag^3L_3) macrocyclic ring. In this macrometalacycle, the lengths of the sides are almost equivalent (9.2–9.5 Å), and the intermetallic separations of Ag···Ag are about 15.7 Å, which are slightly shorter than those of **8**·2 benzene. As shown in Figure 8, two of these honeycomb-like, simple-sheet nets are linked into a 2D double layer through interpolymer Ag–N coordinative interactions (Ag1–N1′ and Ag1′–N1) if dimer coordination (see Figure 7, left) is taken into account. The view along the *b* axis (Figure 8, right) displays these double layers, which are additionally linked by Ag···Ag (d^{10}–d^{10} closed shell) interactions with the cluster anions leading to infinite $^1_\infty[Ag^{I+}]$ chains along [100]. Interestingly, to enable such Ag_{cation}···$Ag_{cluster-anion}$ interactions, the tetrameric $[Ag_4(CF_3CO_2)_6]^{2-}$ cluster ion must adopt a highly distorted structure (especially around Ag2), as illustrated in Figure 7. Evidently, this severe deformation results from strong interactions of the guest cluster anions to the cationic host networks, which is a rare example of the host cationic networks containing guest cluster anions.[43] In $[Ag_3(TCPA)(CF_3CO_2)_3]_n$ nCH_2Cl_2), no such Ag_{cation}···$Ag_{cluster-anion}$ interactions are found. The tetrameric cluster anion is also much less distorted (see the Supporting Information) and composed of four silver(I) ions and six trifluoroacetate anions, in which the four Ag^{+} ions are bridged by carboxylate groups alternately above and below

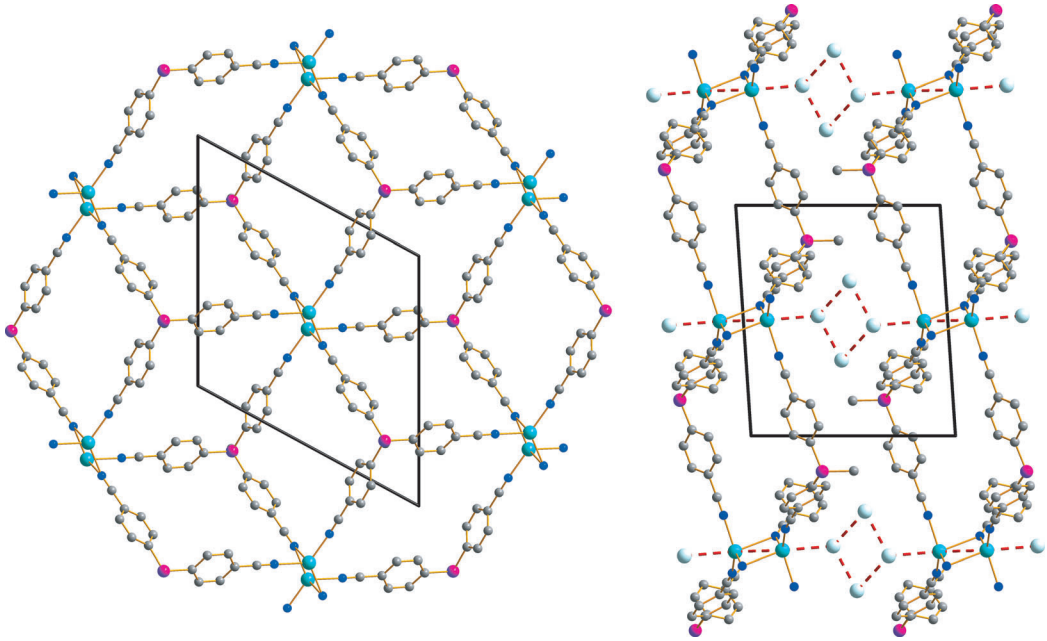

Figure 8. View of the cationic 2D network in $^2_\infty\{[Ag\{MeSi(p\text{-}C_6H_4CN)_3\}]_2\}^{2+}$ along the *a* axis (left). Cluster anion $[Ag_4(O_2CCF_3)_6]^{2-}$, hydrogen atoms and solvent molecules are omitted for clarity. Right: View long the *b* axis, the four Ag centers (light blue) of the cluster anion are included to demonstrate the interaction of the cluster anion with the cationic framework, leading to infinite Ag···Ag chains (dotted red line).

the Ag_4-plane (Scheme 3, species G). In this discrete tetranuclear silver cluster anion (Figure 7, right), each Ag^+ ion is a distorted triangle coordinated by three oxygen atom from the three $CF_3CO_2^-$ anions with Ag–O distances ranging from 2.185(5) to 2.324(2) Å (cf. 2.201(5) to 2.345(5) Å in $[Ag_3(TCPA)(CF_3CO_2)_3]_n$ nCH_2Cl_2).[43] In each Ag_4O_{12} moiety, the four Ag^+ ions are linked by six μ^2-$CF_3CO_2^-$ anions. The Ag···Ag distances range from 2.9708(3) to 3.033(3) Å (cf. 2.956–3.072 Å in $[Ag_3(TCPA)(CF_3CO_2)_3]_n \cdot nCH_2Cl_2$), which are significantly shorter than the sum of the van der Waals radii of two silver atoms (see above). Notably, there are numerous weak C_{aryl}–H···F_{anion} and C_{aryl}–H···O_{anion} van der Waals interactions that fix the benzene molecules in the cavities. Additionally, such stabilizing interactions are also found between the cationic framework and the cluster anions.

In the next series of experiments, we studied the influence of the noncoordinating substituent attached to the silicon atom. For this reason, PhSi(*p*-$C_6H_4CN)_3$ and cycHexSi(*p*-$C_6H_4CN)_3$ were prepared. With the PhSi($C_6H_4CN)_3$ linker, we were able to synthesize the OTf and TFA silver salts. Because the data set of the single-crystal X-ray study of $^2_\infty${[Ag{PhSi(*p*-$C_6H_4CN)_3$}]-[O_3SCF_3]·benzene} (**10**·benzene) was poor, we have only discussed the topology, but not the distances and angles, in detail. Compound **10**·benzene crystallizes in the triclinic space group $P\bar{1}$ with two formula units per cell. Voids are filled with benzene molecules (one per formula unit). As shown in Figure 9, the (distorted) tetrahedral coordination of each Ag^+ ion consists of three nitrogen atoms from three distinct PhSi(*p*-$C_6H_4CN)_3$ ligand molecules and one oxygen atom from the triflate group; a situation that is similar to **8**·2benzene. Although all nitrogen atoms of the MeSi(*p*-$C_6H_4CN)_3$ ligand are involved in the binding of Ag^+ ions, leading to a 2D network, the triflate anion acts as monodentate ligand and two oxygen atoms remain uncoordinated. Starting from the distorted trigonal AgN_3 unit (Figure 9), each PhSi(*p*-$C_6H_4CN)_3$ ligand links three silver atoms to generate an infinite honeycomb cationic network. Thus, in contrast to the interpenetrated 3D network in **8**·2benzene, in which a methyl group is replaced with a phenyl group (as in **10**·benzene), only a 2D network is formed (Figure 10 versus Figure 6). The honeycomb-like macrometalacycles are composed of 6 Si–CN–C_6H_4–Ag moieties in contrast to 5 in **8**·2benzene, which leads to a 48-membered heterocycle. In addition, each infinite honeycomb network forms a double layer with a second one, with weakly interacting triflate and phenyl groups, as illustrated in Figure 10 (left). Between such double layers, no significant interactions were observed (Figure 10, right).

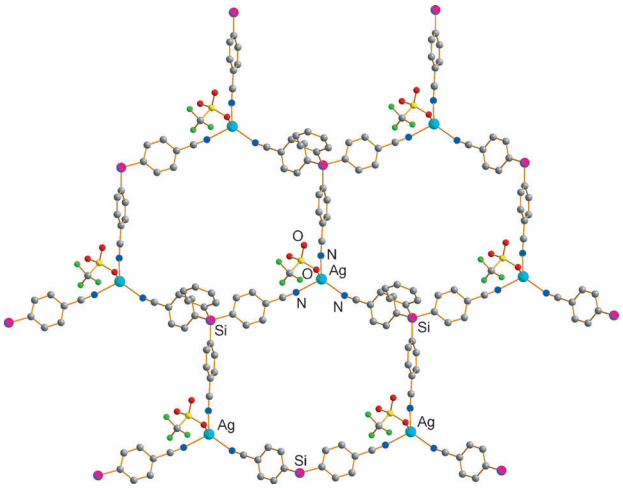

Figure 9. View of the cationic 2D network in $\mathbf{10}^+$. Hydrogen atoms and solvent molecules are omitted for clarity.

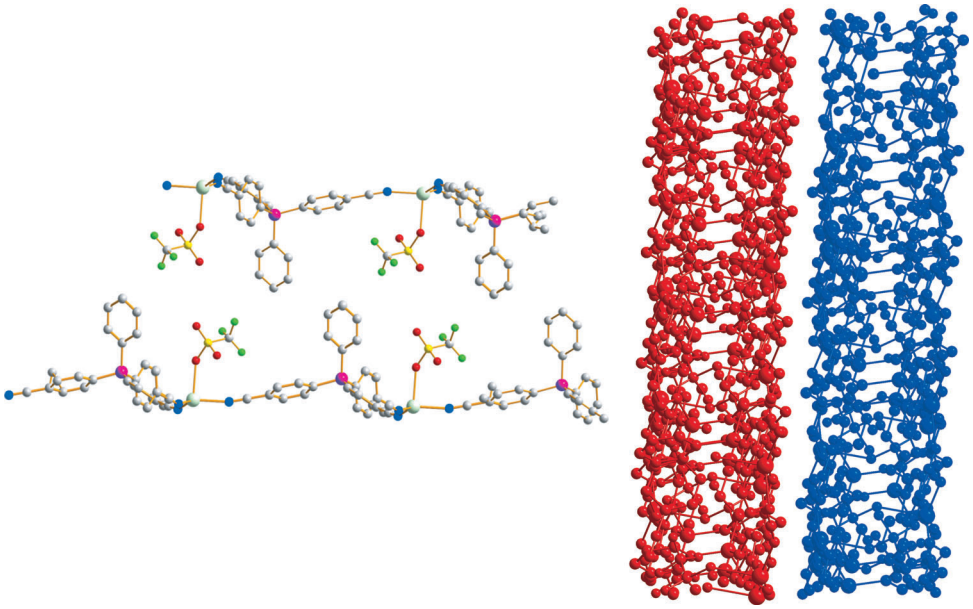

Figure 10. Left: View of a section of a double layer in $^2_\infty${[Ag{PhSi(*p*-$C_6H_4CN)_3$}][O_3SCF_3]. Right: Two double layers. Hydrogen atoms and solvent molecules are omitted for clarity.

$^3_\infty${[Ag{PhSi($C_6H_4CN)_3$}]O_2CCF_3 (**11**) crystallizes in the tetragonal space group $P4_32_12$ with eight formula units per unit cell. In contrast to **10**·benzene, treatment of AgTFA with PhSi(*p*-$C_6H_4CN)_3$ led to a compact 3D network without solvent molecules because no voids formed. The most prominent structural feature is the formation of $Ag_2(O_2CCF_3)_2L_2$ (L = PhSi(*p*-$C_6H_4CN)_3$) dimers. Adjacent silver atoms are joined in a bridging fashion by two TFA groups; thus giving rise to $Ag_2(O_2CCF_3)_2L_2$ dimers, which are identical to those found in the structure of the TFA silver salt[49] (Figure 11 and Scheme 3, species D). Both silver atoms have a distorted tetrahedral coordination, are surrounded by two oxygen atoms of two distinct $[O_2CCF_3]^-$ ions (Ag–O

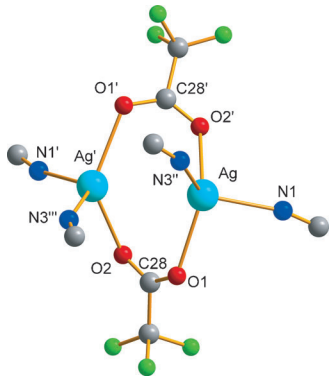

Figure 11. $Ag_2(O_2CCF_3)_2L_2$ (L = PhSi(*p*-$C_6H_4CN)_3$) dimer in **11**. Symmetry codes: ′: *x*, −*y*, *z*; ″: −0.5 + *x*, 0.5 − *y*, −0.25 + *z*; ‴: −0.5 + *x*, 0.5 − *y*, 0.25 − *z*.

2.354(8), 2.293(6) Å), and are linked to two nitrogen atoms from different PhSi($C_6H_4CN)_3$ linkers (Ag–N 2.279(6), 2.291(5) Å). The Ag···Ag′ contact distance is 3.173(1) Å, which is shorter than the sum of the van der Waals radii. Interestingly, although **11** forms a dense 3D network, only two of the CN groups of the linker connect silver dimers, whereas the third remains uncoordinated (Figure 12).

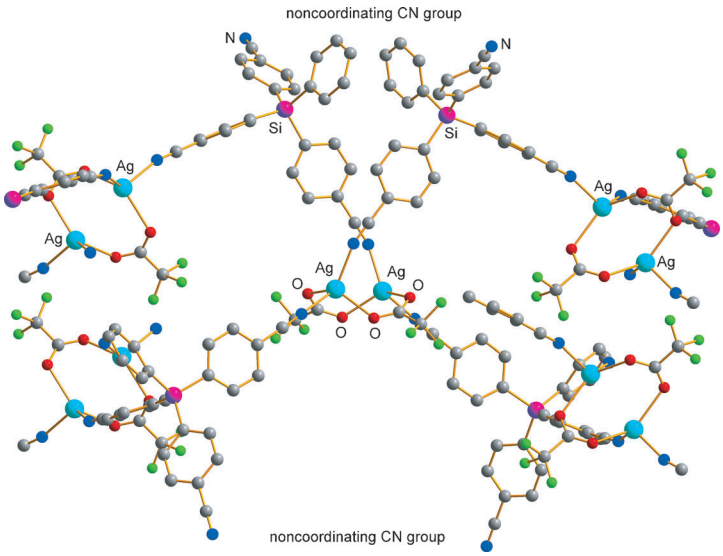

Figure 12. Section of the 3D network in **11**, which highlights coordination of the Ag_2 dimers and the noncoordinating CN groups. Hydrogen atoms are omitted for clarity.

Finally, we used the cycHexSi(*p*-$C_6H_4CN)_3$ ligand in the reaction with AgOTF in benzene and obtained a 2D layer structure with a honeycomb-like structural motif (Figure 13). $^2_\infty${[Ag{cycHexSi($C_6H_4CN)_3$}][O_3SCF_3]·benzene} (**12**·benzene) crystallizes in the orthorhombic space group $P2_12_12_1$ with four formula units in the unit cell. The structure of complex **12** is comprised of (6,3) layers of hexagonal meshes, with alternating three-connected Ag^I centers and tridentate cycHexSi($C_6H_4CN)_3$ ligands (Figure 13). The layers are highly undulated and composed of 42-membered Ag^3L_3 macrocycles (L = cycHexSi(*p*-$C_6H_4CN)_3$. Cross-linking between the macrocycles, which leads to the formation of a 2D network (Figure 13), is achieved by one cyano group per cycHexSi(*p*-$C_6H_4CN)_3$ ligand. The triflate counterion only acts as a monodentate ligand. In this macrometalacycle, the length of the sides are about 15.3 (transannular Ag···Si distance) and 15.1 Å (transannular Ag···Ag distance), that is, the size of the window is smaller than those in **8**·2 benzene (29.7/16.7 Å) and **10**·benzene (19.0/15.6 Å). Nevertheless, the structure resembles that of **10**·benzene, although no double layers are formed (Figure 10) owing to the absence of directing weak F···H–C_{aryl} interactions. Hence, as depicted in Figure 13 (right), two independent interpenetrating networks are observed.

Coordination around the silver centers is distorted tetrahedral with three CN groups of three different ligands (Ag–N 2.10(2)–37(2) Å) and an oxygen atom of a triflate counteranion (Ag–O1 2.388(9) Å; cf. Ag–O2 4.19(1) and Ag–O2 3.71(1) Å). The bond angles around silver are in the range of 87.0(3)–126.2(2) (O-Ag-N) and 106.34(8)–122.27(8)° (N-Ag-N).

Coordination polymers with the tetradentate ligand Si(p-$C_6H_4CN)_4$

As early as 1997, Tilley and Liu reported on the structures of silver coordination polymers with the tetradentate ligand Si(*p*-$C_6H_4CN)_4$ and the counterions $CF_3SO_3^-$ and PF_6^-.[30] Si(*p*-$C_6H_4CN)_4$ crystallized with $AgCF_3SO_3$ from benzene and dichloromethane to give [Ag_2Si(*p*-$C_6H_4CN)_4$]-[CF_3SO_3]$_2$·2 benzene (**15**·2 benzene). The extended solid structure is composed of interpenetrating double layers which are three-connected through trigonal planar silver and tetrahedral silver centers.[30] Because our studies on coordination polymers with RSi($C_6H_4CN)_3$ and R_2Si($C_6H_4CN)_2$ revealed large differences between $AgCF_3SO_3$- and $AgCF_3CO_2$-based coordination polymers (see above), it seemed interesting to treat a solution of $AgCF_3CO_2$ in benzene with Si(*p*-$C_6H_4CN)_4$. Indeed, crystals of isolated $^3_\infty${[Ag_4{Si(*p*-$C_6H_4CN)_4$}]($O_2CCF_3)_4$}·3 benzene (**14**·3 benzene) displayed, contrary to **15**·2 benzene reported by Tilley and Liu,· a diamond-like 3D network (Figure 14).

Compound **14**·3 benzene crystallizes in the monoclinic space group *C*2/*c* with four formula units per cell with three independent silver ions. Two CN groups of each Si(*p*-$C_6H_4CN)_4$ coordinates Ag^+ centers (Ag3) in a monodentate fashion (Figure 15), whereas the two remaining CN groups bind to Ag1 and Ag2 in a bridging fashion through μ_2-N1. It is worthwhile mentioning that the Ag–N distances of bridging N1 are significantly different (μ_2-N1: Ag1–N1 2.272(5) and Ag2–N1 2.664(9) Å): one is short and in the range of the monodentate Ag–N distance (Ag3–N2 2.233(4) Å), whereas the other is considerably longer, but still much shorter than the sum of the van der Waals radii (cf. Σ_{vdW}(Ag···N) = 3.27 versus Σ_{cov}(Ag–N) = 1.99 Å).[34,44] As depicted in Figure 16, the coordination sphere around the silver ions is different. Whereas Ag1 and Ag3 bind to two nitrogen and two oxygen atoms and have near-tetrahedral geometry with bond angles between 94.8(3) and 122.4(2)°, the Ag2 ion is almost T-shaped and sur-

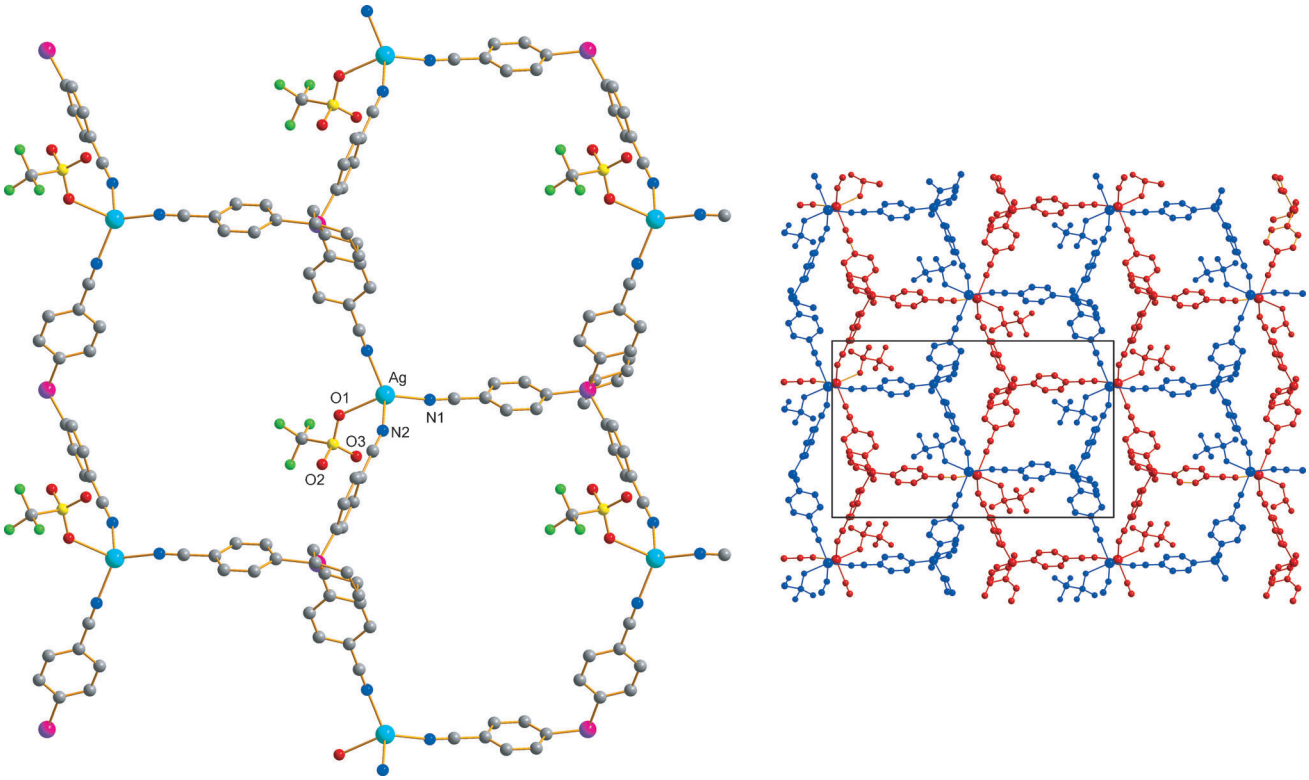

Figure 13. Left: Front view of a section of a single layer in **12**·benzene. Right: View along the *a* axis of the twofold interpenetrated layers. Hydrogen atoms are omitted for clarity.

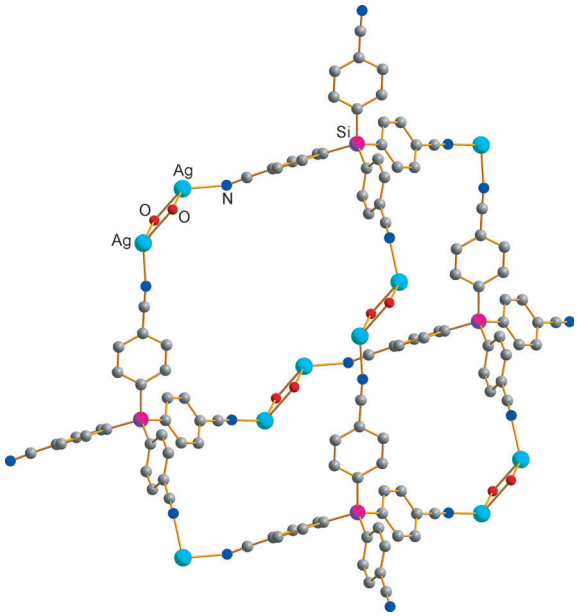

Figure 14. Adamantane motif in **14**·3 benzene. (Structure reduced to this motif.)

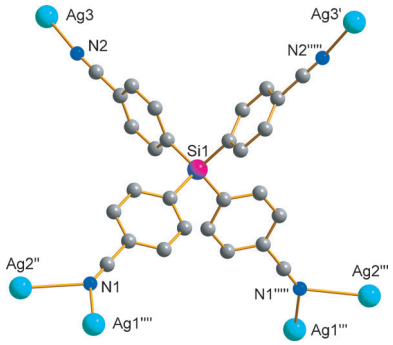

Figure 15. Coordination modes of the $Si(C_6H_4CN)_4$ ligand. Symmetry codes: ′: 1+*x*, *y*, 1+*z*; ″: 0.5−*x*, −0.5+*y*, 1.5−*z*; ‴: 0.5+*x*, −0.5+*y*, *z*; ⁗: 0.5+*x*, −0.5+*y*, 1+*z*; ′′′′′:1−*x*, *y*, 1.5−*z*.

rounded by three oxygen atoms (O2-Ag2-O3 89.9(1), O2-Ag2-O4 106.5(1), O3-Ag-O4 156.3(2)°), and, in addition, one weaker coordination mode is found with one nitrogen atom (Ag2-μ_2-N1 2.664(9) Å). Thus, the coordination sphere seems to be best described by a [3 O + 1 N + 1 Ag] mode, leading to a distorted bisphenoidal geometry around Ag2. Compared with **15**·2 benzene, the triflate anion plays an integral part in deciding the structure around the silver ions, as illustrated in Figure 16. The TFA ion adopts different coordination modes (cf. Scheme 3): 1) Ag1 and Ag3 are bridged by one O1 atom of two different TFA ions to form a planar four-membered Ag_2O_2 dimer (Ag1–O1 2.284, Ag3–O1 2.366(3) Å). The remaining oxygen atom of both TFA ions (O2) binds to Ag2 (Ag2–O2 2.392 Å); thus leading to the formation of an undulated six-membered Ag_2CO_2N heterocycle (if the bridging N1 atom is also taken into account), which is condensed into the dimer. 2) In addition, two Ag2 ions are bridged by two chelating TFA ions through O3 and O4 (Ag2–O3 2.219(4), Ag2–O4 2.207(4) Å), resulting in the

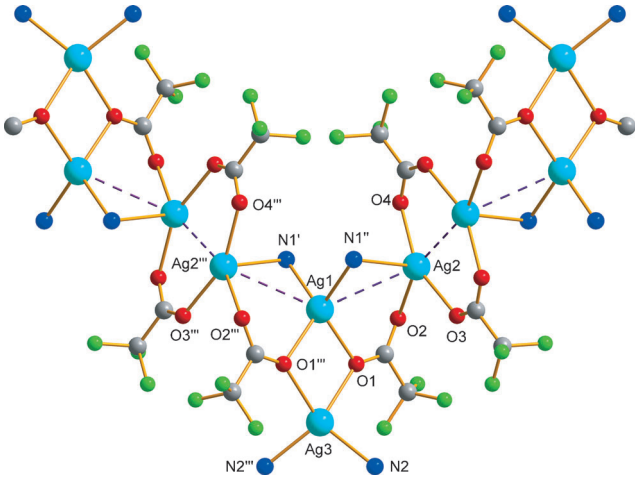

Figure 16. The coordination sphere around the different Ag^+ centers in **14**·3 benzene. Phenyl rings are omitted for clarity. Dashed lines between Ag^+ centers (Ag···Ag < 3.304 Å) indicate infinite Ag···Ag chains along the *c* axis. Symmetry codes: ′: −0.5+*x*, 0.5+*y*, −1+*z*; ″: 0.5−*x*, 0.5+*y*, 1.5−*z*; ‴: −*x*, *y*, 0.5−*z*.

formation of an planar eight-membered $Ag_2C_2O_4$ heterocycle, which is also directly associated with two five-membered rings. Hence, a chain of connected four-, six-, and eight-membered silver-containing heterocycles is formed along the *c* axis. As indicated by the dashed lines in Figure 16, the transannular Ag···Ag distances (five-membered ring: Ag1···Ag2 3.3039(4) Å, eight-membered ring: Ag2···Ag2′ 2.9512(7) Å) are shorter than the sum of the van der Waals radii (Σ_{vdW}(Ag···N) = 3.4 Å), which indicates significant argentophilic interactions[50] along the *c* axis. The Ag···Ag distance within the four-membered ring amounts to 3.5024(7) Å, which is slightly larger; however, a chain of silver-containing heterocycles is also formed when the five- and eight-membered rings are exclusively considered. Furthermore, all of these heterocycles discussed are part of an adamantoid network, also known as a super-diamondoid structure.[42] This long-range structure consists of edge-sharing adamantoid units (Figure 14), which are composed of four silicon, two silver, and four Ag_2O_2 (dimers) nodes cross-linked by 12 *p*-C_6H_4CN linkers. Additionally, twofold interpenetration is observed (Figure 17). The two "independent" networks interpenetrate in such a way that each tetrahedral node is found at the center of an adamantane unit of the other framework, and the four connections to nearest neighbors project through the four cyclohexane-like windows of the surrounding adamantane unit (Figure 17).[51] Strictly speaking, neither networks is independent in **14**·3 benzene because both networks are linked by $Ag_2[CF_3CO_2]_2$ dimers, as illustrated in Figure 17. Interpenetration in adamantoid networks is a common feature.[52] A known exception to this observation is the intriguing example of $^3_\infty${[Cu(4,4′,4″,4‴-tetracyanotetraphenylmethane]·BF_4·*x*$C_6H_5NO_2$}, which exists as a single adamantoid array with no interpenetration, reported by Robson and Hoskins.[39a,53]

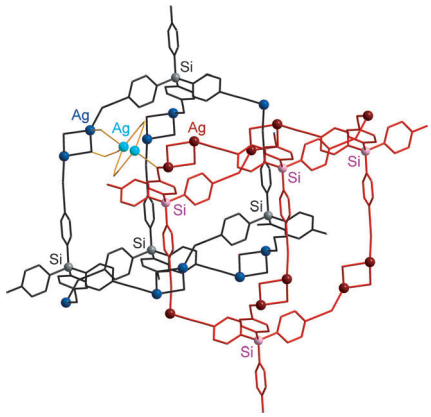

Figure 17. Two interpenetrating adamantane moieties of two independent diamond-like nets linked by $Ag_2[CF_3CO_2]_2$ dimers (only one linkage is shown; structure reduced to this motif).

Conclusion

We presented a general synthesis for different *p*-cyanophenylsilanes and their application as bi-, tri, and tetradentate ligands in the coordination chemistry of Ag^IX (X = OTf, TFA) and the coordinating behavior of these compounds in silver coordination polymers. The topology of the network changed with variation of the denticity, with the coordination strength of the anion, and also with the variation of the nonfunctional part of the tridentate ligand. Although the OTf anion only weakly bound to the Ag^+ ions, and thus, strengthened the Ag–N bonds, the TFA anion mediated the tuning of the structure of the motifs by utilizing different coordination modes (Scheme 3). This often led to silver (cluster) anions with close Ag···Ag distances[43] or even silver chains,[16,38,54] which were part of 2D and 3D networks, depending on the denticity of the *p*-cyanophenylsilane. Clearly, the [AgL_n]TFA salts forced the Ag^+ ions to approach each other (in contrast to the OTf ion) and were therefore excellent examples suitable for the study of metallophilic attractions with ligands supported in closed-shell Ag^I systems.[55] Coordination polymers with Ag···Ag interactions may possess electrical semiconductive properties.[9] The [AgLn]OTf solid-state structures with the weaker coordinating OTf ion were mainly influenced by the denticity and nonfunctionalized substituent (Me, Ph, cycHex) of the *p*-cyanophenylsilane. $^1_\infty${[Ag{$Me_2Si(C_6H_4CN)_2$}]}O_2CCF_3·0.5 CH_2Cl_2} forms double-stranded chains, $^3_\infty${[Ag{$MeSi(C_6H_4CN)_3$}]}·O_3SCF_3·2 benzene} forms a 3D network built from 70-membered Ag^5L_5 macrocycles, and $^2_\infty${[Ag{$PhSi(C_6H_4CN)_3$}][O_3SCF_3]·benzene} and **12**·benzene form an infinite honeycomb cationic 2D network. No close Ag···Ag distances were observed for any of the triflate silver salts. In the future, it will be interesting to see whether we can make use of classic weakly coordinating anions, such as BF_4^- or larger $B(C_6F_5)_4^-$, to display nearly exclusive ligand–metal interactions.

Keywords: coordination modes · coordination polymers · salt effect · silver · X-ray diffraction

[1] C.-T. Chen, K. S. Suslick, *Coord. Chem. Rev.* **1993**, *128*, 293 – 322.
[2] Y.-B. Dong, G.-X. Jin, M. D. Smith, R.-Q. Huang, B. Tang, H.-C. Loye, *Inorg. Chem.* **2002**, *41*, 4909 – 4914.
[3] S. Noro, M. Kondo, T. Ishii, S. Kitagawa, H. Matsuzaka, *J. Chem. Soc. Dalton Trans.* **1999**, 1569 – 1574.
[4] J. W. Han, K. I. Hardcastle, C. L. Hill, *Eur. J. Inorg. Chem.* **2006**, 2598 – 2603.
[5] T. K. Maji, R. Matsuda, S. Kitagawa, *Nat. Mater.* **2007**, *6*, 142 – 148.
[6] O. M. Yaghi, H. Li, C. Davis, D. Richardson, T. L. Groy, *Acc. Chem. Res.* **1998**, *31*, 474 – 484.
[7] A. R. Millward, O. M. Yaghi, *J. Am. Chem. Soc.* **2005**, *127*, 17998 – 17999.
[8] A. G. Wong-Foy, J. A. Matzger, O. M. Yaghi, *J. Am. Chem. Soc.* **2006**, *128*, 3494 – 3495.
[9] C. Janiak, *Dalton Trans.* **2003**, 2781 – 2804.
[10] A. M. Withersby, A. J. Blake, N. R. Champness, P. Hubberstey, W.-S. Li, M. Schröder, *Angew. Chem.* **1997**, *109*, 2421 – 2423; *Angew. Chem. Int. Ed. Engl.* **1997**, *36*, 2327 – 2329.
[11] E. D. Genuis, J. A. Kelly, M. Patel, R. McDonald, M. J. Ferguson, G. Greidanus-Strom, *Inorg. Chem.* **2008**, *47*, 6184 – 6194.
[12] A. Lamann-Glees, U. Ruschewitz, *Cryst. Growth Des.* **2012**, *12*, 854 – 861.
[13] Y. B. Dong, H.-X. Xu, J.-P. Ma, R.-Q. Huang, *Inorg. Chem.* **2006**, *45*, 3325 – 3345.
[14] L. Li, S. Wang, T. Chen, Z. Sun, J. Luo, M. Hong, *Cryst. Growth Des.* **2012**, *12*, 4109 – 4115.
[15] D. Tanaka, S. Kitagawa, *Chem. Mater.* **2008**, *20*, 922 – 931.
[16] X. L. Lu, W. K. Leong, L. Y. Goh, A. T. S. Hor, *Eur. J. Inorg. Chem.* **2004**, 2504 – 2513.
[17] J. Harloff, H. Lund, A. Schulz, A. Villinger, *Z. Anorg. Allg. Chem.* **2013**, *639*, 754 – 764.
[18] J. Harloff, M. Karsch, H. Lund, A. Schulz, A. Villinger, *Eur. J. Inorg. Chem.* **2013**, 4243 – 4250.
[19] K. Voss, M. Becker, A. Villinger, V. N. Emel'yanenko, R. Hellmann, B. Kirchner, F. Uhlig, S. P. Verevkin, A. Schulz, *Chem. Eur. J.* **2011**, *17*, 13526 – 13537.
[20] A. Bernsdorf, H. Brand, R. Hellmann, M. Köckerling, A. Schulz, A. Villinger, K. Voss, *J. Am. Chem. Soc.* **2009**, *131*, 89588970.
[21] P. Sengupta, H. Zhang, D. Y. Son, *Inorg. Chem.* **2004**, *43*, 1828 – 1830.
[22] D. Wang, H. He, X. Chem, S. Feng, Y. Niu, D. Sun, *CrystEngComm* **2010**, *12*, 1041 – 1043.
[23] H. N. Peindy, F. Guyon, I. Jourdain, M. Knorr, D. Schildbach, C. Strohmann, *Organometallics* **2006**, *25*, 1472 – 1479.
[24] B. Wang, *Coord. Chem. Rev.* **2006**, *250*, 242 – 258.
[25] J. W. Lee, E. A. Kim, Y. J. Kim, Y.-A. Lee, Y. Pak, O.-S. Jung, *Inorg. Chem.* **2005**, *44*, 3151 – 3155.
[26] C. Rim, H. Zhang, D. Y. Son, *Inorg. Chem.* **2008**, *47*, 11993 – 12003.
[27] J. B. Lambert, Z. Liu, C. Liu, *Organometallics* **2008**, *27*, 1464 – 1469.
[28] See reference [21].
[29] W. H. Yim, L. M. Tran, E. E. Pullen, D. Rabinovich, L. M. Liable-Sands, T. E. Concolino, A. L. Rheingold, *Inorg. Chem.* **1999**, *38*, 6234 – 6239.
[30] F.-Q. Liu, T. D. Tilley, *Inorg. Chem.* **1997**, *36*, 5090 – 5096.
[31] C. A. van Walree, X. Y. Lauteslager, A. M. A. van Wageningen, J. W. Zwikker, L. W. Jenneskens, *J. Organomet. Chem.* **1995**, *496*, 117 – 125.
[32] W. E. Parham, L. D. Jones, *J. Org. Chem.* **1976**, *41*, 1187 – 1191.
[33] H. Jacobsen, H. Berke, S. Doering, G. Kehr, G. Erker, R. Froehlich, O. Meyer, *Organometallics* **1999**, *18*, 1724 – 1735.
[34] P. Pyykkö, M. Atsumi, *Chem. Eur. J.* **2009**, *15*, 12770 – 12779.
[35] See reference [10].
[36] D. Venkataraman, G. B. Gardner, A. C. Covey, S. Lee, J. S. Moore, *Acta Crystallogr. Sect. C* **1996**, *52*, 2416 – 2419.
[37] O. M. Yaghi, H. Li, *J. Am. Chem. Soc.* **1996**, *118*, 295 – 296.
[38] M. O. Awaleh, A. Badia, F. Brisse, X.-H. Bu, *Inorg. Chem.* **2006**, *45*, 1560 – 1574.
[39] a) B. F. Hoskins, R. Robson, *J. Am. Chem. Soc.* **1990**, *112*, 1546 – 1554; b) H. S. Zhdanov, *Acad. Sci. URSS* **1941**, *31*, 352 – 354; c) T. Kitazawa, S. Nishikiori, R. Kuroda, T. Iwamoto, *J. Chem. Soc. Dalton Trans.* **1994**, 1029 – 1036.
[40] O. Ermer, *J. Am. Chem. Soc.* **1988**, *110*, 3747 – 3754.
[41] R. Robson, B. F. Abrahams, S. R. Batten, R. W. Gable, B. F. Hoskins, J. Liu in *Supramolecular Architecture: Synthetic Control in Thin Films and Solids* (Ed.: T. Bein), American Chemical Society, Washington DC, **1992**, pp. 256 – 273.
[42] A. J. Blake, N. R. Champness, S. S. M. Chung, W.-S. Li, M. Schroder, *Chem. Commun.* **1997**, 1005 – 1006.
[43] J. Ni, K.-J. Wie, Y. Liu, X.-C. Huang, D. Li, *Cryst. Growth Des.* **2010**, *10*, 3964 – 3976.
[44] A. Bondi, *J. Phys. Chem.* **1964**, *68*, 441 – 451.
[45] a) K.-J. Wei, J. Ni, J. Gao, Y. Liu, Q.-L. Liu, *Eur. J. Inorg. Chem.* **2007**, 3868 – 3880; b) L. Carlucci, G. Ciani, P. Macchi, D. M. Proserpio, S. Rizzato, *Chem. Eur. J.* **1999**, *5*, 237 – 243.
[46] a) P. Reiss, F. Weigend, R. Ahlrichs, D. Fenske, *Angew. Chem.* **2000**, *112*, 4085 – 4089; *Angew. Chem. Int. Ed.* **2000**, *39*, 3925 – 3929; b) L. Zhao, X.-L. Zhao, T. C. W. Mark, *Chem. Eur. J.* **2007**, *13*, 5927 – 5936; c) L. Zhao, T. C. W. Mark, *Organometallics* **2007**, *26*, 4439 – 4448; d) L. Zhao, W.-Y. Wong, T. C. W. Mark, *Chem. Eur. J.* **2006**, *12*, 4865 – 4872.
[47] S. Banfi, L. Carlucci, E. Caruso, G. Ciani, D. M. Proserpio, *Cryst. Growth Des.* **2004**, *4*, 29 – 32.
[48] D. Venkataraman, S. Lee, J. S. Moore, P. Zhang, K. A. Hirsch, G. B. Gardner, A. C. Covey, C. L. Prentice, *Chem. Mater.* **1996**, *8*, 2030 – 2040.
[49] R. G. Griffin, J. D. Ellett, Jr., M. Mehring, J. G. Bullitt, J. S. Waugh, *J. Chem. Phys.* **1972**, *57*, 2147 – 2155.
[50] M. Dennehy, O. V. Quinzani, R. A. Burrow, *Acta Crystallogr. Sect. C* **2007**, *63*, m395 – m397.
[51] S. R. Batten, R. Robson, *Angew. Chem.* **1998**, *110*, 1558 – 1595; *Angew. Chem. Int. Ed.* **1998**, *37*, 1460 – 1494.
[52] A. J. Blake, N. R. Champness, P. Hubberstey, W.-S. Li, M. A. Withersby, M. Schröder, *Coord. Chem. Rev.* **1999**, *183*, 117 – 138.
[53] a) B. F. Hoskins, R. Robson, *J. Am. Chem. Soc.* **1989**, *111*, 5962 – 5964.
[54] Yu. V. Kokunov, Yu. E. Gorbunova, V. V. Kovalev, *Zh. Neorg. Khim.* **2008**, *53*, 2016 – 2023; *J. Inorg. Chem.* **2008**, *53*, 1885 – 1892.
[55] M. Jansen, *Angew. Chem.* **1987**, *99*, 1136 – 1149; *Angew. Chem. Int. Ed. Engl.* **1987**, *26*, 1098 – 1110.
[56] CCDC 994414 (**2**), 994415 (**3**), 994416 (**4a**), 994417 (**4b**), 994418 (**5a**), 994419 (**5b**), 994420 (**6**), 994421 (**7**), 994422 (**8**), 994423 (**11**), 994424 (**12**), 994425 (**13**), 994426 (**14**) contain the supplementary crystallographic data for this paper. These data can be obtained free of charge from The Cambridge Crystallographic Data Centre via www.ccdc.cam.ac.uk/data_request/cif.

Received: February 19, 2014
Published online on April 8, 2014